DOE/ EML-391

AN ITERATIVE NONLINEAR UNFOLDING CODE: TWOGO

Ferenc Hajnal

Environmental Measurements Laboratory
U. S. Department of Energy
New York, New York 10014

March 1981

Printed in the United States of America
Available from
National Technical Information Service
U. S. Department of Commerce
5285 Port Royal Road
Springfield, VA 22161

NTIS price codes
Printed copy: $6.00
Microfiche copy: A01

ABSTRACT

A new iterative unfolding code, TWOGO, was developed to analyze Bonner sphere neutron measurements. The code includes two different unfolding schemes which alternate on successive iterations. The iterative process can be terminated either when the ratio of the coefficient of variations in terms of the measured and calculated responses is unity, or when the percentage difference between the measured and evaluated sphere responses is less than the average measurement error. The code was extensively tested with various known spectra and real multisphere neutron measurements which were performed inside the containments of pressurized water reactors.

TABLE OF CONTENTS

INTRODUCTION

Numerous Bonner sphere neutron measurements were performed to characterize neutron fields inside pressurized water reactor (PWR) containments for neutron dosimetry purposes[1, 2]. A code, TWOGO, which utilizes two different unfolding methods was developed to obtain approximate solutions of the neutron spectral distribution from a limited number of measurements. The Gold[3] and Scofield[4] iterative techniques are identical and can be applied with some success to unfold Bonner sphere neutron measurements[2], therefore they were selected as one of the methods. The second is Twomey's[6] iterative nonlinear unfolding technique. The latter is applied to a mathematically identical problem, the indirect estimation of particle size distributions from a limited number of measurements of the number of particles transmitted through filters with known filtration characteristics. Both methods provide nonzero and positive solutions, on the condition that the initial estimates are also nonzero and positive.

The simultaneous use of two different methods in one unfolding code is somewhat unique. The selection of the two methods used here is based on extensive numerical experimentation and computer tests, which indicate that the two methods when used in conjunction provide faster convergence and more stable solutions of multisphere measurements than by using only one or the other of the methods. Moreover, a somewhat novel arresting condition is applied in the unfolding code, and a part of that arresting condition is built into the first algorithm. The TWOGO code is short and the unfolding time is reasonable, only 3 minutes per spectrum on the IBM 360-60 or 1.5 sec on the CDC-6600 computers. This advantage might make the present code applicable to microcomputers, where the length of the code and fast convergence are essential.

The determination of a physically appropriate neutron spectral distribution is a formidable problem since in this case the neutron spectral information in 26 energy intervals is attempted to be obtained from as few as six measurements. Also, in practice, multisphere neutron measurements have varying and occasionally very poor counting statistics, such as 50% (one standard deviation) in an extreme case. If thermoluminescence detectors are used in place of a single ^{6}LiI(Eu) scintillator, as the thermal neutron detector at the center of the Bonner spheres, neutron spectral and intensity variations may occur over the extended location where the seven detector system is spread out. This may cause variations in the individual detector response in excess of the expected experimental errors. Also, incorrect subtraction of the unwanted accumulated TL signal during handling and transit can cause serious errors.

To extract a physically appropriate solution when lacking sufficient measurements, a priori conditions are utilized; these pertain to the smoothness of the derived spectrum, a rapidly declining differential neutron flux at the high energy end of the spectrum, the knowledge of the general shape of the trial vector, and a positive nonzero solution. Extensive computer tests with experimental data,

as well as pseudo and perturbed pseudo measurements show that the present unfolding code performs very well provided proper arresting conditions and trial vector are used. The spectral results are very good for up to 10% random measurement errors, are good for up to 20% random errors, and are quite acceptable for up to 50% errors. The integral quantities, such as neutron flux and dose-equivalent rates are accurate within ±20% even for 50% random errors. These accuracies can be considered acceptable for routine neutron dosimetry purposes.

NEUTRON SPECTRAL DETERMINATION

The use of a few spherical moderators with thermal neutron detectors at their centers to determine the neutron spectral distribution in a wide energy range, in an unknown field, was suggested by Bonner in 1960[6]. The system consists of a few, 6 - 11, spherical polyethylene moderators with $^{6}LiI(Eu)$ or $^{10}BF_3$ proportional counters at their centers which measure the (n, α) reaction rates. The true counting rate, Y_i, measured with the i^{th} Bonner sphere is defined as

$$Y_i = \int_0^\infty R_i(E)\varphi(E)dE, \tag{1}$$

where $R_i(E)$ is the response function of the i^{th} Bonner sphere and $\varphi(E)$ is the true differential neutron flux. The experimentally determined counting rates, B_i, are subject to the errors, $\bar{\epsilon}_i$, and cannot be expected to be equal to Y_i, which is to say that

$$B_i = Y_i + \bar{\epsilon}_i. \tag{2}$$

Since the detector response functions, $R_i(E)$, are known only in group averaged and discretized form, with matrix elements A_{ij}, Equation 1 is rewritten in discretized form as the set of quadrature formulae,

$$B_i = \sum_{j=1}^{n} A_{ij}F_j\Delta E_j + \epsilon_i, \qquad i = 1, \ldots, m \tag{3}$$

where m is the number of detectors, n is the number of energy intervals, ϵ_i is the combined experimental measurement and response matrix errors, and F_j is the differential neutron flux in energy interval j. A consequence of the conversion to quadrature formulae, when n is small and the energy intervals are wide, is that the solution vector $\vec{F}$ for the neutron spectral distribution, even when all

$\epsilon_i = 0$, will only approximate the true differential neutron flux $\varphi(E)$. Therefore the scope of this report is not to solve Equation 1 for $\varphi(E)$, but rather to obtain approximation of it in the form of $\vec{F}$. Since the number of discretization or mesh points, n, is larger than the number of response functions, that is the number of Bonner spheres, m, the solution of the discretized equations, Equation 3, is not unique. In practice, approximate mathematical techniques and a priori conditions may be used to extract physically acceptable solutions. Another source of nonuniqueness is that, even if all $\epsilon_i = 0$, the finite resolution of the experimental device destroys some of the information in the true differential neutron flux, $\varphi(E)$, such as the effects of closely spaced resonance absorption[7]. Generally, at least for dosimetric purposes, a solution vector, $\vec{F}$, is acceptable if the calculated detector responses corresponding to $\vec{F}$ are in good agreement with the experimental responses. Furthermore, certain minimum conditions have to be satisfied, such as the sum of the error squares, Q (as obtained from Equation 3 by substituting the solution vector $\vec{F}$ obtained yet in an undefined way) which has a minimum value and can be written as

$$\min Q = \frac{1}{m} \sum_{i=1}^{m} \epsilon_i^2 \tag{4}$$

The energy range of the neutron field in the PWR containment with fission spectra as sources covering 10 decades and the selected energy intervals of the response matrix A of Equation 3 are distributed fairly uniformly on a logarithmic scale. Therefore, it is convenient to express the energy on a logarithmic scale, and in the case of the TWOGO code, in base 10. The lethargy here is defined by the integral form

$$u = \log (E/1 \text{ MeV}),$$

that is

$$E = 10^u, \tag{5}$$

or the differential form

$$dE = \ln 10 \, E du. \tag{6}$$

The true differential flux $\varphi(E)$ can be obtained in terms of neutron flux per unit lethargy, C(u),

$$\varphi(E) = C(u) \frac{du}{dE} = C(u)/(\ln 10 \, E) \tag{7a}$$

or the discretized differential neutron flux, F_j, in terms of discretized C_j,

$$F_j = C_j \frac{\Delta u_j}{\Delta E_j}, \qquad j = 1, \ldots, n. \tag{7b}$$

Then Equation 3 can be written as

$$B_i = \sum_{j=1}^{n} A_{ij} C_j \Delta u_j + \epsilon_i, \qquad i = 1, \ldots, m. \tag{8}$$

To extract a physically acceptable solution, $\vec{C}$, which also satisfies Equation 4, or a similar requirement, two recursion formulae are applied. First, according to Twomey's procedure, one starts with a trial vector, $\vec{C}^0$, whose general shape is the same as $\vec{C}(u)$, the true solution of Equation 1. At each iteration, the previous solution is modified over the entire region where the response function is nonzero, and the $(\ell + 1)^{th}$ estimate of C_j is

$$C_j^{\ell+1} = \left[1 + K_i \left(\frac{B_i}{B_i^*} - 1\right) \frac{A_{ij}\Delta u_j}{\max(A_{ik}\Delta u_k)}\right] C_j^{\ell}$$

$$\begin{aligned} i &= 1, \ldots, m \\ j &= 1, \ldots, n \\ k &= 1, \ldots, n \end{aligned} \tag{9}$$

where

$$B_i^* = \sum_{j=1}^{n} A_{ij} C_j^{\ell} \Delta u_j, \qquad i = 1, \ldots, m \tag{10}$$

is the calculated response of the i^{th} Bonner sphere in terms of the trial or the previous solution vector $\vec{C}^{\ell}$.

The scaling factors K_i in Equation 9 have two purposes, namely:

1. K_i regulates the rate of convergence and prevents oscillation, and
2. K_i may include a weighting factor, w_i,

$$w_i = \frac{\min(P_i)}{P_i} \tag{11}$$

to obtain

$$K_i = K w_i, \quad i = 1, \ldots, m \tag{12}$$

where $K = 0.5$ and P_i is the one standard deviation error associated with the i^{th} sphere measurement, $\min(P_i)$ being the minimum value of these errors, i.e. the error of the best measurement.

The introduction of a weighting factor is an addition to Twomey's recursion formulae. The modification of the previous solution vector, $\vec{C}$, is repeated in sequence for all the m detectors, preferably in order of increasing statistical accuracy.

While using Twomey's algorithm no restrictions are placed on the random error components, on the other hand, the Gold[3] and Scofield[4] algorithms, which are incorporated into the present code, only evolved from "the application of this method to an exact problem"[3]. Therefore, let all $\varepsilon_i = 0$, and using

$$A_{ij}\Delta u_j = G_{ij} \qquad i = 1, \ldots, m, \qquad j = 1, \ldots, n$$

rewrite Equation 8 in matrix form.

$$\vec{B} = G\vec{C} \tag{13}$$

$$G^T\vec{B} = G^TG\vec{C} \tag{14}$$

or

$$\vec{V} = Z\vec{C} \tag{15}$$

where

$$Z = G^TG.$$

The pseudo inverse

$$A^* = (G^TG)^{-1}\, G^T \tag{16}$$

results in a solution of

$$\vec{C} = A^*\vec{B} \tag{17}$$

which is not unique since $m < n$. There are more unknowns than equations in Equation 13, which is called the underdetermined case, and Equation 13 has an infinite number of least square solutions. The solution is the best in a least-square sense and is of minimum length[8].

When the rank of a matrix is very high, as in this case, the determination of A^* is not very practical and an iterative technique can replace the direct matrix inversion method and still obtain a solution for $\vec{C}$. The Gold and Scofield algorithm offers an alternate solution of $\vec{C}$ from Equation 15. Starting with a trial solution, the approximation to $\vec{C}$ is obtained at each (k + 1) iteration via the recursion formula,

$$C_j^{k+1} = C_j^k V_j \Big/ \sum_{i=1}^{n} \mathbb{R}_{ji} C_j^k \qquad j = 1, \ldots, n, \tag{18}$$

where $C_j^k = C_j^{\ell+1}$ of Equation 9.

These algorithms, Equations 9 and 18, are repeated until min Q (specified later) is found, or a point is reached where the rate of convergence is so poor that any further iteration is of little value.

It was observed when using only the Gold and Scofield recursion relation that the convergence might not be monotonic at all times and an occasional local minimum might precede the true minimum[1, 3]. This was manifested in the failure of an arresting condition which simply required that the residue, S, defined as

$$S = \sum_{i=1}^{m} (B_i - B_i^*)^2 ,$$

reaches a minimum value. In the TWOGO code, to avoid the termination of the iteration after such an occurrence, the test for the minimum is performed on the mean value, Q_1, of two average absolute fractional differences of the last eight or twelve iterations. The new test quantity min Q_1 is defined as

$$\min Q_1 = (P_a^n + P_b^n)/2, \tag{19a}$$

where P_a^n is given by

$$P_a^n = \frac{1}{m} \sum_{i=1}^{m} \left| 1 - \frac{B_i^*}{B_i} \right| \tag{19b}$$

and is the average absolute fractional difference between the measured and calculated responses in terms of the measured sphere counts, and P_b^n is given by

$$P_b^n = \frac{1}{m} \sum_{i=1}^{m} \left| \frac{B_i}{B_i^*} - 1 \right| \qquad (19c)$$

and is the average absolute fractional difference between the measured and calculated responses in terms of the calculated sphere responses. The values of Q_1, P_a^n, and P_b^n can be converted to percentage values by simply multiplying the quantities by 100. These percentage values of these quantities will often be used instead of the fractional values.

There is a close relationship between the value of P_b^n and the correction term of Twomey's algorithm, Equation 9. According to this term, convergence is reached for the i^{th} detector if $B_i/B_i^* = 1$. Due to the measurement errors of B_i, simultaneous convergence cannot be expected or achieved for all m detectors simultaneously. It is not unreasonable, however, to expect that in the case of statistically good measurements both P_a^n and P_b^n, or even the sum of them also will reach a minimum value in the neighborhood of the same number of iterations, which is expressed above by Equation 19a.

The condition for terminating the iterations can be further improved if, in conjunction with Q_1, a second test quantity, here called the convergence criterion, Q_2, defined by

$$Q_2 = 1 - \frac{P_a^{nn}}{P_b^{nn}} , \qquad (20a)$$

also reaches minimum or optimal value. P_a^{nn} is the coefficient of variation between the measured and calculated sphere responses, and is

$$P_a^{nn} = \sum_{i=1}^{m} \left(1 - \frac{B_i^*}{B_i}\right)^2 \qquad (20b)$$

similarly P_b^{nn} is

$$P_b^{nn} = \sum_{i=1}^{m} \left(\frac{B_i}{B_i^*} - 1\right)^2 \qquad (20c)$$

The supposition that min Q_a is a good arresting condition is based on the following arguments. Starting out with a reasonable trial vector, $\vec{C}^0$, the convergence per iteration near a physically acceptable solution should be uniform and both P_a^{nn} and P_b^{nn} must be small and converge to the same quantity. In other words, if m is large enough the fractional differences should have zero mean. Therefore,

a solution vector $\vec{C}$ is acceptable if the ratio P_a^{nn}/P_b^{nn} is equal to unity, or Q_2 zero.

The numerical values of Q_1 and Q_2 during and at the end of the iterations help to qualify the solution vector indicating whether it is acceptable or not. Here four scenarios will be discussed, which based on numerical experimentations can be expanded;

$$Q_1 \gg 0 \qquad |Q_2| \gg 0$$

$$Q_1 \gg 0 \qquad |Q_2| \simeq 0$$

$$Q_1 \simeq 0 \qquad |Q_2| \gg 0$$

$$Q_1 \simeq 0 \qquad |Q_2| \simeq 0$$

and these might indicate:

1. Bad measurement, not a reasonable trial spectrum, too few or too many iterations.

2. Poor quality measurement, however, the solution vector is reasonable and a situation occurred where one of the measurements, say B_k, might also be suspect. If the iterations are continued, oscillation will set in.

3. The trial vector probably is not a good starter or the iterations already have gone too far, and the optimal solution vector already has been passed.

4. The quality of the measurements is good and the solution vector is acceptable.

These ideas are implemented in the computer code and illustrated later in the unfolding of real and pseudo measurements.

A false minimum of Q_1 or Q_2 can be avoided if the following conditions are met. Let T^k denote Q_1 after the k^{th} iteration. Then, using an eight point test, the iteration cycle is stopped if

$$T^{k-7} \geq T^{k-5} \text{ and } T^{k-6} \geq T^{k-4} \text{ and } T^{k-1} \geq T^{k-3} \text{ and } T^{k} \geq T^{k-2}.$$

A more stringent test is the twelve point test. In this case the iteration is terminated if

$$T^{k-11} \geq T^{k-7} \text{ and } T^{k-10} \geq T^{k-6} \text{ and } T^{k-1} \geq T^{k-5} \text{ and } T^{k} \geq T^{k-4}.$$

Generally if min Q_1 is not found, however the value of Q_1 is less than a preset value, say 5%, the unfolding procedure is terminated at 100 iterations, otherwise at 200 iterations. The intermediate results at 100 iterations are also printed.

The selection of trial vector $\vec{C}^o$ will affect the rate of convergence and its choice should depend on the nature of the measurements. To unfold PWR containment neutron measurements, the trial vector may be one of the calculated typical scalar neutron flux spectra emergent from various reactors at midcore plane. Similarly, to unfold cosmic-ray neutron measurements, a 1/E neutron spectrum is a good trial vector.

THE TWOGO TEST RESULTS

The performance of TWOGO was evaluated. The operation and use of the arresting conditions based on the test quantities Q_1 and Q_2, as discussed in the previous section, were tested by unfolding exactly known spectra, such as pseudo multi-sphere neutron measurements based on calculated reactor, accelerator shielding, cosmic ray, fission, and mono-energetic neutron spectra. A set of eight detector pseudo measurements were used in all the tests and the neutron spectra were unfolded into 26 energy bins, from thermal to 25 MeV neutron energies. The test spectra were smooth and continuous as well as mono-energetic to test the rate of convergence. The accuracy of derived quantities such as total neutron flux, average energy and dose, was tested with pseudo measurements having known random measurement errors incorporated into such measurements. These pseudo measurements were generated by random sampling from the cumulative Gaussian distributions. These data sets have mean values of the exact pseudo multisphere detector counts used in the tests, and the standard deviations are taken to be 5, 10, 20, 30 and 50% of the mean values.

The following test spectra were used to generate the pseudo measurements:

1. Homogeneous water - moderated reactor neutron spectrum in the core position (H_2O)[8].

2. Homogeneous water - moderated reactor neutron spectrum in the beryllium reflector position (H_2O - Be)[8].

3. Oak Ridge Health Physics Research Reactor leakage neutron spectrum at 3 m distance from the core (HPRR)[9].

4. Accelerator side-shielding neutron spectrum on the outside of a 2 kg/cm^2 thick iron shield (2 kg Fe)[10].

5. Cosmic-ray neutron spectrum in the atmosphere (COSMIC)[11].

6. Bare ^{252}Cf fission neutron spectrum (^{252}Cf)[12].

7. Monoenergetic neutron sources in any one of channels 1, 3, 9, 15, 18, 22 and 25.

These spectra were used originally to test an unfolding code which uses only the Gold and Scofield algorithm[1, 2].

Exact Pseudo Measurements

In this section the operation of the code is illustrated with pseudo measurements based on exactly known spectra. The unfolding is terminated if min Q_1 is found, or at 200 iterations. In this section the value of the test quantity Q_2 is not used yet to terminate the iterations.

To unfold the exact pseudo measurements to 1% accuracy, that is $Q_1 \leq 1\%$, only ~40 iterations are needed. However, practice showed that about 200 iterations are needed to obtain on the average less than 0.1% deviation among the input and output multisphere counts as measured by Q_1. Such high accuracy has only minor interest in neutron dosimetry, since in practice the statistical errors in the measurement distribution usually have a much larger average relative standard deviation than 0.1%.

The results of unfolded exact pseudo measurements based on the two moderated reactor spectra, H_2O and H_2O - Be, after 100 and 200 iterations respectively, are compared with the true spectra in Figures 1 and 2. The convergence of each of these pseudo measurements is excellent and the average percentage deviations as measured by P_a^n are 0.08 and 0.19. The values of the test quantity Q_2, Equation 20, are 0.00 in both cases, which indicates that the residuals are nearly randomly distributed around a zero mean and the quantities P_a^n and P_b^n are equal. From the progress of the iterations during the unfolding, rapid convergence is observed at the first 20 iterations after which the improvement is less than 0.02% per iteration. The unfolding of the HPRR leakage spectra also produced excellent results, 0.19 average percentage difference as measured by P_a^n and Q_2 is 0.01 at 20 iterations. The integral quantities are reproduced to within 1% or better. The trial vector in all three previous cases was a calculated midcore leakage spectrum of a PWR.

Although not the primary purpose of this code development program, 1/E type neutron spectra were also unfolded. The unfolded results of the accelerator side-shielding and cosmic-ray neutron spectra are compared with the true spectra in Figures 3 and 4. The number of iterations are 115 and 200, respectively. The average percentage errors measured by P_a^n are 0.63 and 0.12, and Q_2 are 0.01 and 0.00. Visual inspection of the progress of the unfolding, that is the value of P_a^n, P_b^n and Q_2 indicated that the unfoldings proceeded smoothly, and the convergence is quite rapid. The unfolded cosmic-ray spectrum shown is obtained at a

very broad local minimum of Q_1 at 115 iterations. Although the convergence resumed again at 130 iterations, there was no significant change by 200 iterations. Both of the unfolded spectra are in very good agreement with the true spectra, even though the small peak in channel 16, corresponding to 17 keV, of the accelerator side shielding spectrum is not exactly reproduced. The trial vector in both cases was a 1/E neutron spectrum.

The accelerator side-shielding and cosmic-ray neutron spectra were also unfolded starting with a reactor-type trial vector. Convergence in both cases was satisfactory. However, the integral quantities, after an equivalent number of iterations as done with the 1/E trial vector, were only accurate to about 4%. The reason for the discrepancy is due to the order of magnitude of the differences between the reactor type trial spectrum and true spectrum in energy bins 24, 25 and 26.

The energy response of neutron detectors and spectrometers is usually calculated, and the detector responses are normalized with the aid of neutron sources whose absolute neutron emission rate and spectral characteristics are known. Such absolute calibrations of neutron spectrometers can be performed with bare ^{252}Cf fission neutron sources and monoenergetic neutron sources. Accordingly, TWOGO was tested with pseudo measurements of ^{252}Cf fission and monoenergetic neutron sources.

In Figure 5 the unfolded results of the exact pseudo ^{252}Cf fission and true neutron spectra are compared. At 200 iterations the agreement in the energy interval from 14 keV to 15 MeV, where more than 99.5% of the total neutron flux is present, is quite good. The integral quantities are reproduced within 2%, and at least 600 iterations would be needed to get better than 1% accuracy. The total flux, however, is accurate to 0.2% after 200 iterations. A slightly moderated fission spectrum was used as the trial vector.

The unfolding of exact pseudo measurements of the various monoenergetic sources converges quite slowly. The selection of a proper trial vector, however, could speed up the convergence. Here the same trial vector was used as in the case of the unfolding of the earlier moderated reactor neutron spectra.

The monoenergetic pseudo measurements in energy bins 1, 3, 9, 15, 22 and 25 were unfolded individually each to 400 and 1200 iterations and are compared in Figure 6 showing the percentage of the neutron flux per energy bin versus energy bin (100% is perfect agreement). Due to the shape of the trial vector, which is a reactor type spectrum, no fast convergence is expected. In unfolding measurements with filtered neutron beams such as scandium or iron, the trial vector should be compatible with the measurements. The total neutron flux and dosimetric quantities after 400 iterations is quite accurate, to within 2%. Only the average energy shows slow convergence, and about 300 iterations are needed to obtain 2% accuracy.

Effects of Random Errors

Next, the effects of known, synthesized random errors were investigated. Each group of test data was randomly perturbed to obtain 5, 10, 15, 20, 30 and 50% standard deviation errors. At first only min Q_1 is required to terminate the iterations, or if no min Q_1 was found, all the iterations proceeded to 200 iterations. These unfoldings of pseudo measurements will illustrate the presence of oscillation in the solution vector when the percentage errors are large and the iterations continue after min Q_2 is found. The same trial vector, the reactor midcore leakage spectra was used as in Figures 1 and 2. No significant spectral distortions were observed in unfolding the slightly perturbed H_2O - Be data with 5 and 10% errors as shown in Figures 7 and 8, both at 200 iterations. The integral quantities also reproduced quite well, to better than 5%. Serious spectrum distortion and oscillation in the unfolded spectra will occur with any data which has more than 10% statistical error if the unfolding proceeds to 200 iterations. In Figure 9 the unfolded results of the test spectrum H_2O - Be with 15%, in Figure 10 with 30%, and in Figure 11 with 50% synthesized errors are compared with the true spectrum, each at 200 iterations. The same data at 100 and at 40 iterations show progressively less spectral distribution.

Next the code was tested with 18 different pseudo measurement data sets, each having synthesized errors. At this time the numerical values of Q_1, Q_2, and P_a^n were visually examined and the following procedure was implemented to extract physically acceptable and numerically stable results and spectral information.

1. All the pseudo measurements were unfolded for 200 iterations. The results were read out at 100 and 200 iterations, and were accepted if Q_1 was smaller, near 100 or 200 iterations. In addition, the convergence has to be smooth, that is both P_a^n and P_b^n have to decline monotonically and the test quantity Q_2 has to be the smallest.

2. If min Q_1 occurs at less than 200 iterations, the unfolding is repeated and terminated at min Q_1, provided min Q_2 is also in the same neighborhood.

3. If no min Q_1 exists and min Q_2 is found, repeat the unfolding and terminate at min Q_2. The number of iterations should be greater than 5.

4. If no min Q_1 and no min Q_2 occurs, and P_a^n is 5 to 10% or greater, a good estimate of the spectra and integral quantities may be obtained around 30 iterations. Also, a new trial vector should be tried and the iterative process should be repeated starting at point 1 above.

5. If no min Q_1 occurs, however, if P_a^n is stabilized or the changes in it are negligible, stop the iterations at that point, since further iterations are not warranted. At the point where P_a^n stabilizes, Q_2 also stabilizes, however,

Q_2 may be a large quantity. A large Q_2 value may indicate bad data. In any case, repeat the unfolding with a different trial vector.

As a general rule, the solution, starting with a specific trial vector, which converges most rapidly and reaches min Q_1 and min Q_2 at the smallest number of iterations should be accepted as the best solution. Also min Q_1 should be compatible with the input error estimate.

Some of the test unfolding results implementing the above procedures are shown in Figures 12 to 15.

Test spectra #2, H_2O - Be, with 30 and 50% random errors, are compared with the true spectra in Figures 12 and 13. The iterations were carried out to 10 and 7 iterations where the Q_2 is zero. In both cases the spectral distributions are quite acceptable. These results can be compared with the previous unfolding of the same data set. The average percentage difference, P_a^n, as defined by Equation 19b, in the case of 30% random error at 200 iterations (Figure 10), is 9.6. On the other hand, at the present 10 iterations where Q_2 is zero (Figure 12), the P_a^n is 11. The convergence ratio defined as

$$CR = Q_2 + 1 \tag{21}$$

is 1.28 and 1.00 for the 200 and 10 iterations.

In the case of 50% random error at 200 iterations, the average percentage difference, P_a^n, is 17 and at the present 7 iterations P_a^n is 17.2. The convergence ratio , CR, is 1.51 and 1.03, respectively. The unfolded and true spectra of these cases are shown in Figures 11 and 13.

Other pseudo measurements having large percentage random errors also can be unfolded and the iterations terminated where test quantity Q_2 is zero, even though no min Q_1 can be found. Both the H_2O and the HPRR pseudo measurements having 50% random errors were unfolded and the iterations terminated at $Q_2 = 0$, which occurred at 7 and 12 iterations, respectively. The spectral results are shown in Figures 14 and 15. The average percentage difference , P_a^n, is 10 and 13, respectively. No convergence of the Q_1 values or P_a^n were found anywhere for 200 iterations. In both cases severe oscillations appear by 200 iterations, resulting in somewhat similar spectral distortion as those that occurred at 50% random error of the H_2O - Be pseudo measurement shown in Figure 11.

Measurements Inside PWR Containments

Seventy measurements at 10 different nuclear power stations have been performed by EML[1, a)]. The PWR's differ in size, design, and construction. The expected neutron exposure rates at the locations studied varied from about 0.1 to

500 mrem/h. In this work, multisphere spectrometer systems equipped with various thermal detectors were used. The counting statistics of the measurements varied from a few percent to about 50%. The error of the TLD-equipped multisphere system measurements was estimated to be 10 to 50%. The expected spectral shapes were considered to be similar to the reactor leakage spectra obtained from various calculations. A typical neutron spectrum has a thermal peak of various intensities followed by a steeper than 1/E distribution, and then a short 1/E distribution. Then, depending on the hardness of the spectrum, the spectrum will decline rapidly.

All the PWR measurements were unfolded with the TWOGO code using the same procedure as described in the previous section on the effect of random errors. Only three examples of the unfolding will be presented here. The unfolding of a measurement with good statistics is shown in Figure 16, which is at NPS-8, location 18. A good convergence was reached after 36 iterations. This spectrum is soft and the average energy is only 41 keV. The next spectrum is at a location outside the personnel entrance hatch of NPS-6, location 7. The counting statistic is very poor at this location. Nonetheless, at 18 iterations the unfolding seems quite reasonable and is shown in Figure 17. A suspected measurement with probably very poor statistics is shown in Figure 18. Even this unfolded spectrum is reasonable.

These reactor measurements were unfolded also using the Gold and Scofield algorithm for 1000 iterations, and some of these results[a] can be compared with the results obtained with the TWOGO code. The results of the unfolding of the measurement made at NPS-8, location 8 are very similar and have the same spectral shapes. The integral quantities, such as total neutron flux and dose-equivalent rates, agree to within 8%. The average percentage difference, P_a^n, is 1.4 for the TWOGO and 0.5 for the Reference 2 unfolding. The measurement performed at NPS-6, location 8, has poor counting statistics and the spectrum of Reference 2 has a flat high energy end. The unfolding of the TWOGO code is shown in Figure 17, and it seems quite reasonable. The convergence ratio , CR, is 0.8ℰ and 1.04, and the average percentage difference , P_a^n, is 3.6 and 3.2 of Reference 2 and the TWOGO code, respectively. The last example, a measurement performed at NPS-5, location 3, cannot be unfolded with the Gold and Scofield method alone without additional background correction. Using the TWOGO code this measurement can be unfolded without any additional background correction, and is shown in Figure 18. The CR is unity and P_a^n is 4.8.

Error Estimates

Direct calculation of the error propagation through the iterative processes in the TWOGO code is not possible. Some estimates of the errors involved were obtained from numerical experiments and test unfoldings performed with the TWOGO code. To estimate the errors of the derived integral quantities, such as neutron flux and dose equivalent, about 100 numerical experiments were performed using

both exact and perturbed pseudo measurements, and the deviations of the integral quantities of the perturbed measurements were compared with the output average sphere count errors given by P_a^n. Also, the maximum statistical error of the input counts and the output average sphere count errors, again given by P_a^n, were compared. Although this is by no means a rigorous error estimation, the following useful observations can be made.

a. The maximum value of the statistical error of the input multisphere counts is four times the average percentage error based on the P_a^n of Equation 19b.

b. The deviation of the total flux and dose-equivalent rate from the true values are three times the average percentage error based on P_a^n of Equation 19b.

CONCLUSION

An iterative unfolding computer code was written using two different unfolding schemes on alternate iterations. The primary purpose of the development was to unfold in containment PWR neutron measurements using as few as six Bonner sphere detectors. Since the number of detectors is much smaller than the energy bins, and the measurement errors can be significant, a priori conditions are used to help to extract physically meaningful results.

The running of the code requires the user to have some familiarity with spectral unfolding methods, and their limitations, such as the fact that instead of exact answers only good spectral approximations can be obtained. The user also has to have some idea from physical considerations or calculations of the general shape of the expected neutron spectra. The starting of the code required a trial spectrum which is available from the literature. The user also might generate a trial spectrum based on the knowledge of the neutron field. The best solution is considered to be at a point during the iterations where the absolute fractional differences are compatible with the input measurement errors, and the ratio of the coefficient of variations, in terms of the measurement and calculated sphere responses, is unity. If the ratio of the coefficient of variations is greater or less than unity then either the input data or the code performance, or both may be of questionable value. In such cases the unfolding of the data should be repeated with a different trial vector to identify possible errors in the input data, or the insufficiency of the unfolding code.

The computer code was extensively tested with pseudo and real measurements of reactor, fission source, and cosmic-ray types of neutron spectra. The computer code performs very well in all situations, and the integral quantities, such as neutron flux and dose, are accurate within ±20%, even for 50% random errors in

the measurements. The unfolded neutron spectral information is good for up to 30% random errors in the measurements.

The TWOGO code was used to unfold, with two exceptions, all the PWR neutron measurements, and also the calibration and intercalibration data without introducing any "correction" of the input data, or without rejection of any of the measured sphere counts of the input data sets. All the PWR measurements, which are listed in Reference 2, were unfolded and the results are available.

ACKNOWLEDGEMENTS

The author expresses his appreciation for useful discussions with Harold Beck, James E. McLaughlin and Earl Knutson and his thanks to Keran O'Brien and Robert Sanna of this Laboratory for some of the test data.

REFERENCES

1. Hajnal, F., Sanna, R. S., Ryan, R., and Donnelly, E. H.
   Stray Neutron Fields in the Containment of PWRs, p. 397
   In: International Symposium on Occupational Radiation Exposure in Nuclear Fuel Cycle Facilities (IAEA-SM-242/24), Vienna (1979)

2. Sanna, R. S., Hajnal, F., McLaughlin, J. E., Gulbin, J. F., and Ryan, R. M.
   Neutron Measurements Inside PWR Containments
   USDOE Report EML-379, September (1980)

3. Gold, R.
   An Iterative Unfolding Method for Response Matrices
   USAEC Report ANL-6984 (1964)

4. Scofield, N. E.
   A Technique for Unfolding Gamma-Ray Scintillation Spectrometer Pulse-Height Distribution
   U. S. Navy Report USNRDL-TR-447 (1960)

5. Twomey, S.
   Comparison of Constrained Linear Inversion and an Iterative Nonlinear Algorithm Applied to the Indirect Estimation of Particle Size Distribution
   J. Comput. Phys. 18, 188 (1975)

6. Bramblett, R. L., Ewing, R. I., and Bonner, T. W.
   A New Type of Neutron Spectrometer
   Nucl. Instr. Methods 9, 1 (1960)

7. Burrus, W. R., and Verbinski, V. V.
   Fast-Neutron Spectroscopy with Thick Organic Scintillators
   Nucl. Instr. Methods 67, 181 (1969)

8. Gelb, A.
   Applied Optimal Estimation, Chapter 2, p. 19
   The M.I.T. Press, Cambridge, MA (1974)

9. Moteff, J.
   Reactor Neutron Dosimetry in Irradiation of Materials
   Attix, F. H. and Tochilin, E., Editors
   In: Radiation Dosimetry, Vol. III, Sources, Fields, Measurements and Applications
   Academic Press, New York (1969)

10. Poston, J. W., Knight, J. R., and Whitesides, G. E.
Calculations of the HPRR Neutron Spectrum for Simulated Nuclear Accident Conditions
Health Phys. 26, 217 (1979)

11. O'Brien, K.
Neutron Spectra in the Side-Shielding of a Large Particle Accelerator
USAEC Report HASL-240 (1971)

12. Hess, W. N., Canfield, E. H., and Lingenfelter, R. E.
Cosmic Ray Demography
J. Geophys. Res. 66, 665 (1961)

13. Green, L.
Transmission Measurements of the ^{252}Cf Fission Neutron Spectrum
Nucl. Sci. Eng. 37, 232 (1969)

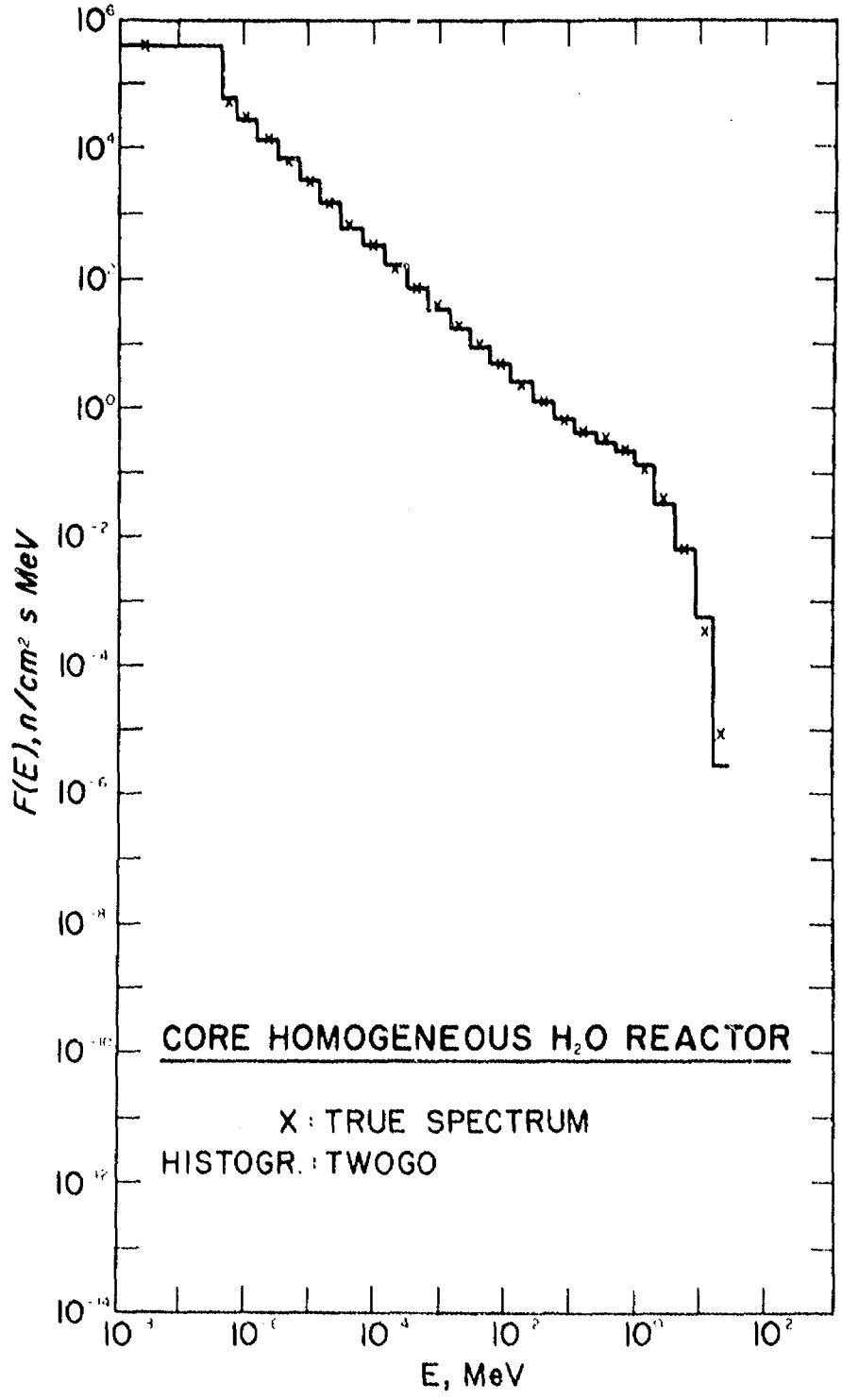

Figure 1. The true and unfolded neutron spectrum in midcore of a homogeneous H_2O reactor, $Q_2 = 0$, 100 iterations.

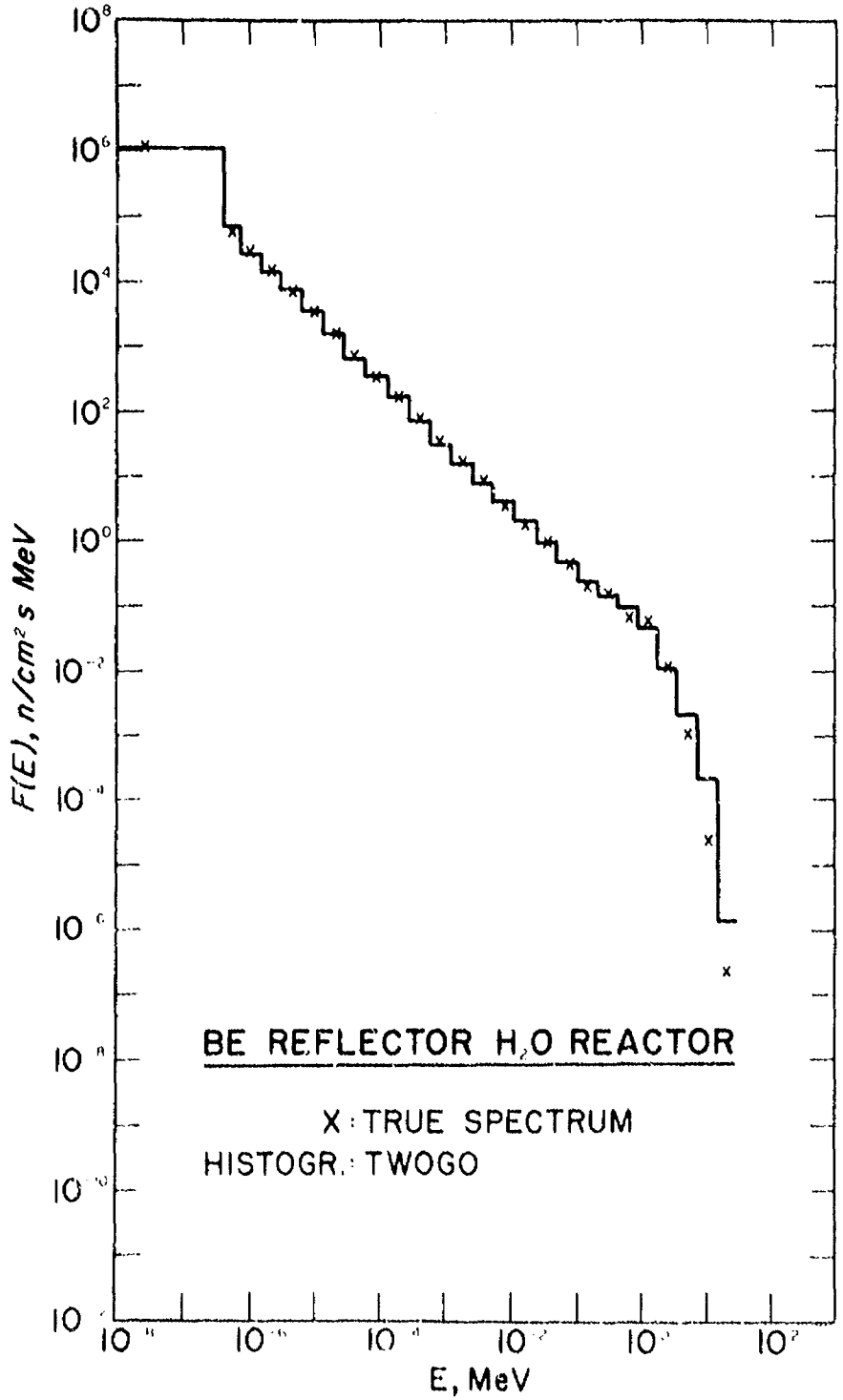

Figure 2. The true and unfolded neutron spectrum in the Be reflector of a homogeneous H_2O reactor, $Q_a = 0$, 200 iterations.

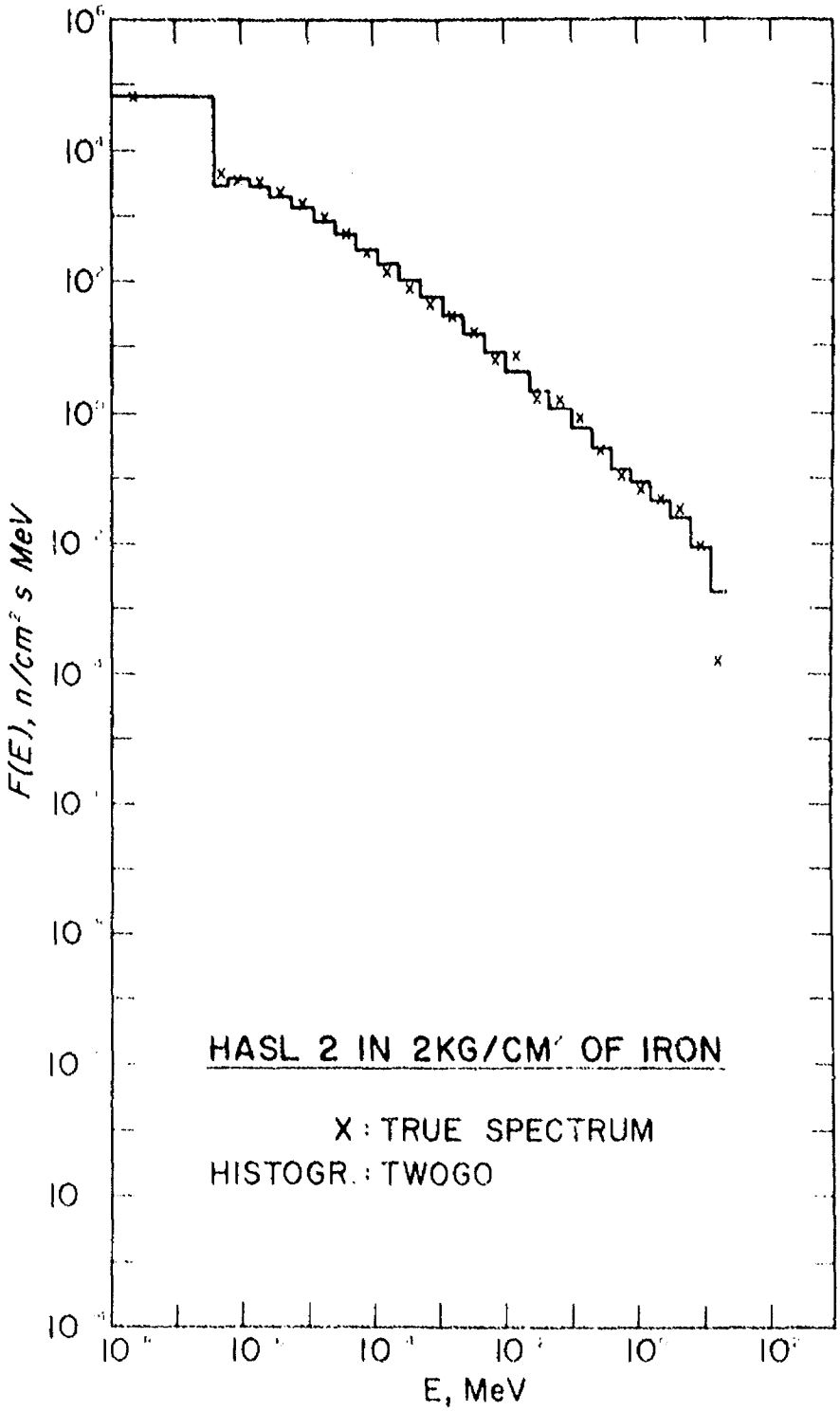

Figure 3. The true and unfolded neutron spectrum of an accelerator side shielding at 2 kg/cm² depth of a 2 kg/cm² thick iron shield, Q_a = 0, 200 iterations.

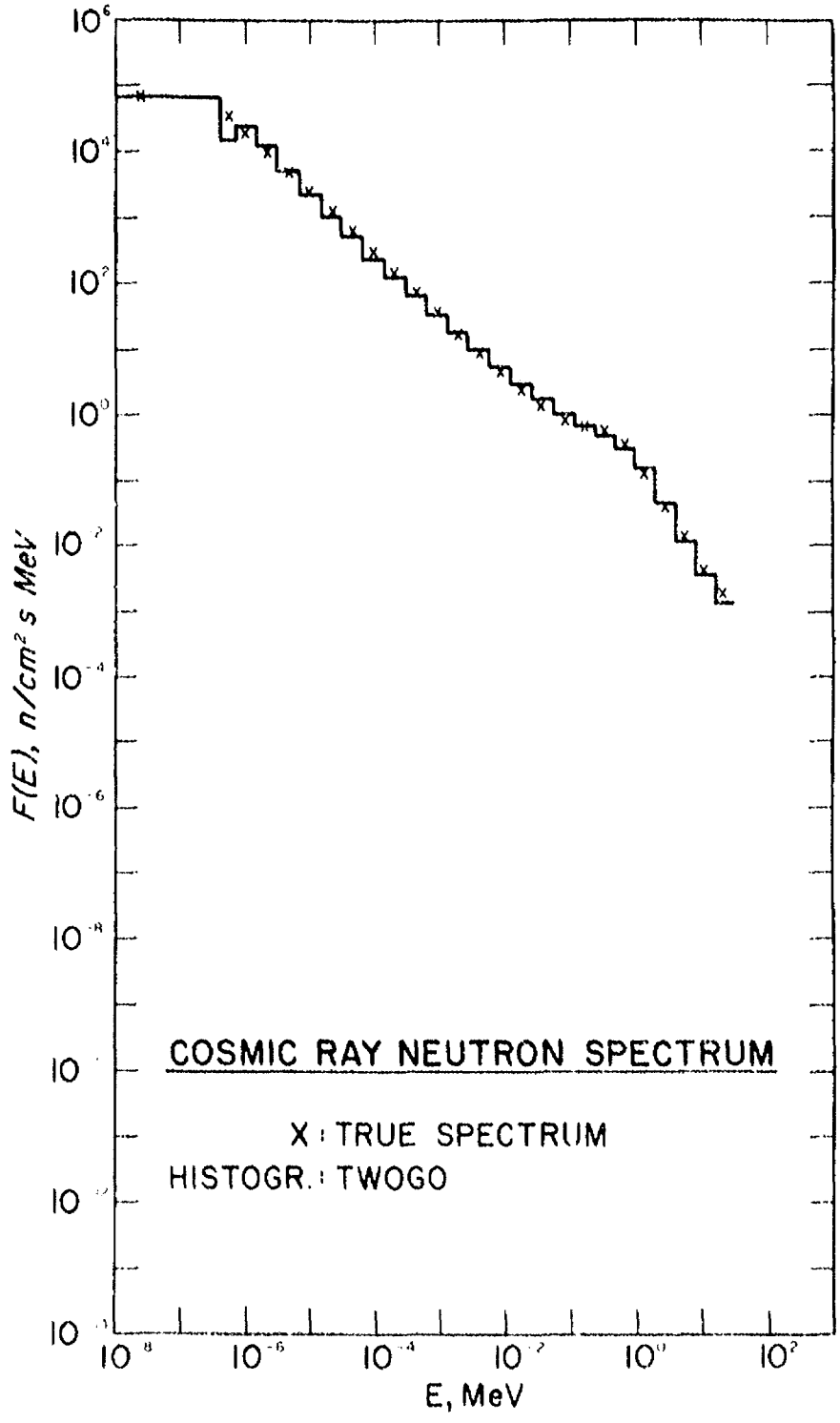

Figure 4. The true and unfolded cosmic-ray neutron spectrum, $Q_2 = 0$, 115 iterations.

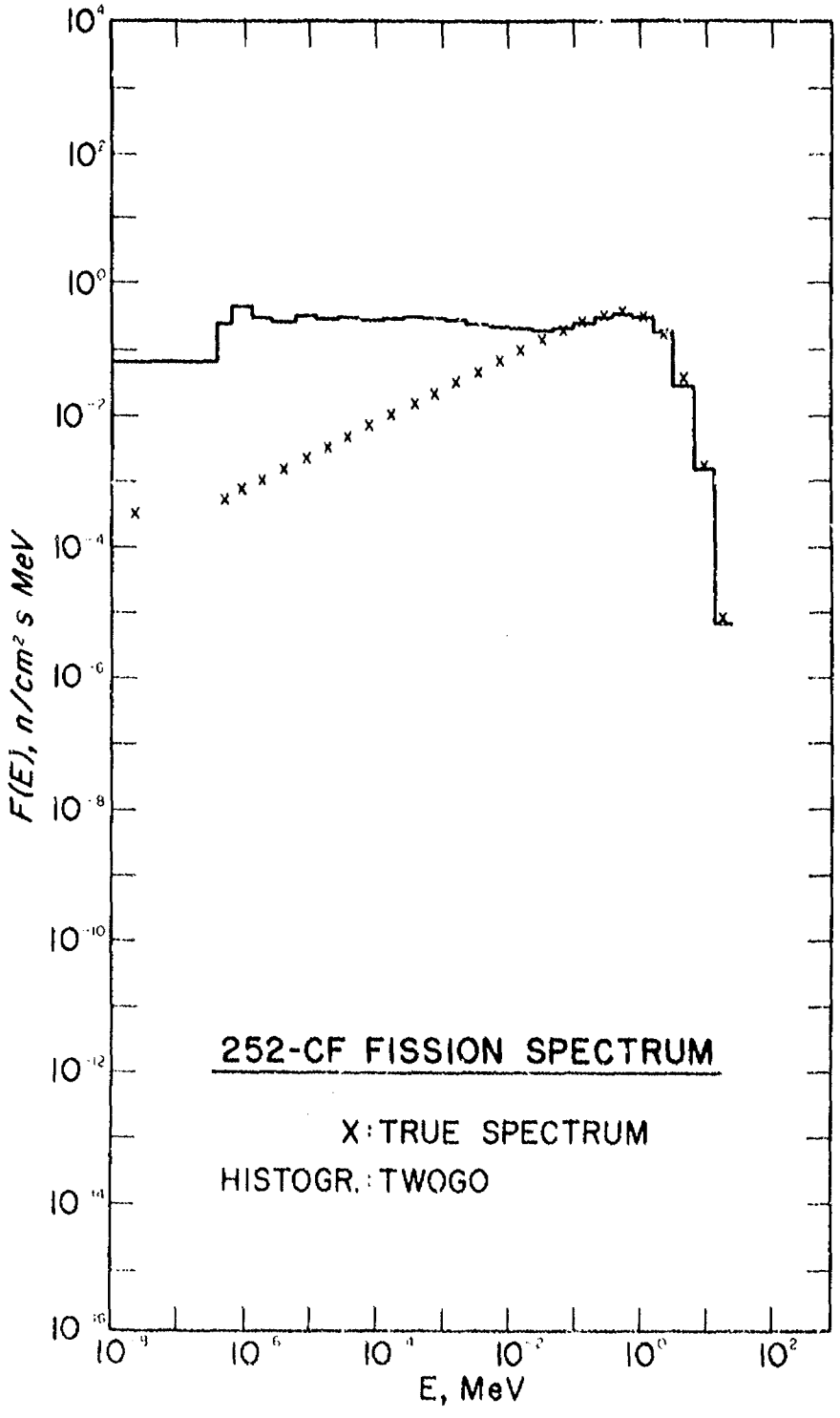

Figure 5. The true and unfolded neutron spectrum of a ^{252}Cf fission source, Q_a = 0, 200 iterations.

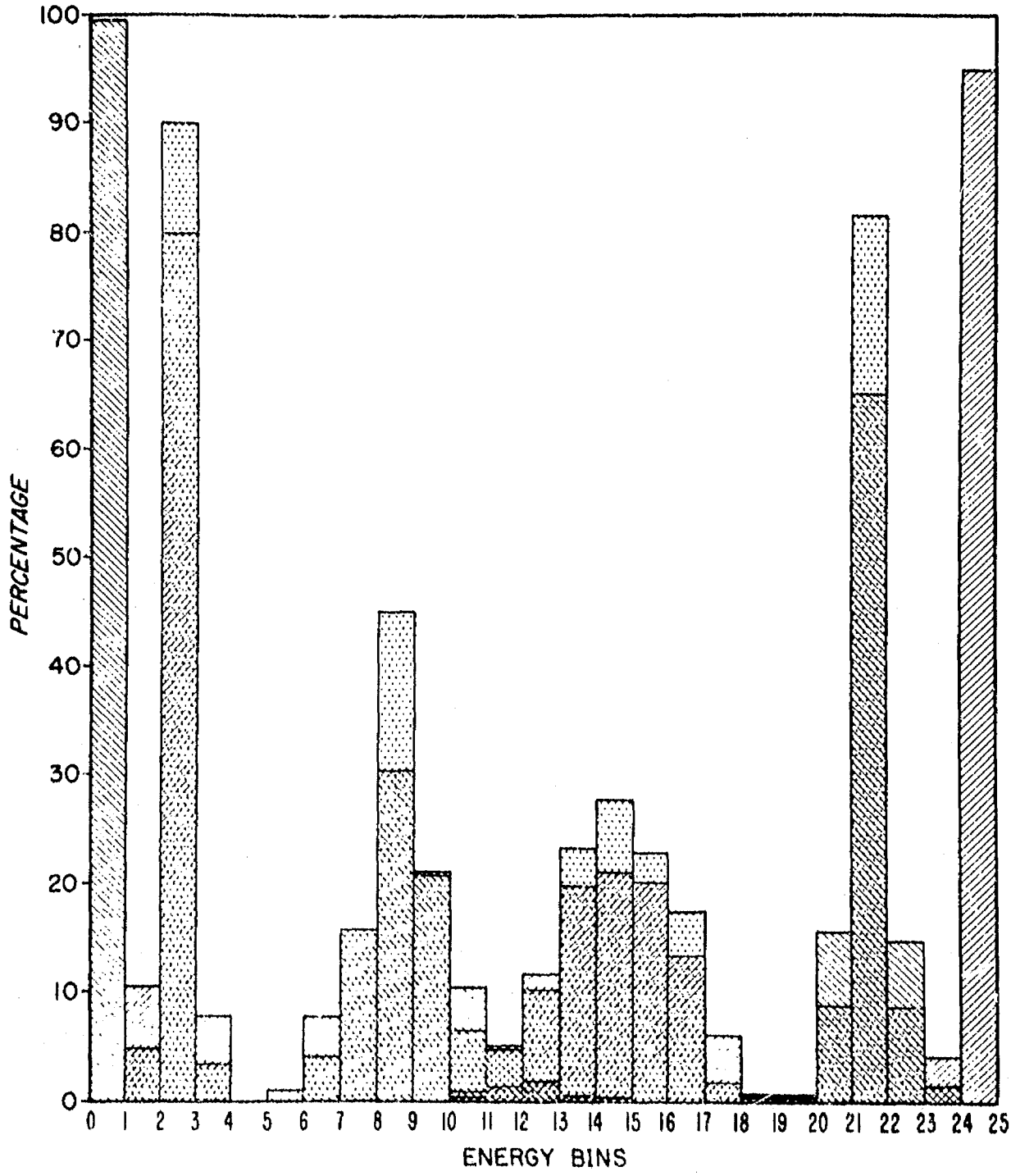

Figure 6. The individually unfolded pseudo neutron measurements of monoenergetic sources in energy bins 1, 3, 9, 15, 22 and 25. The number of iterations is 400 and 1200. Percentage of neutron flux versus energy bins are shown. Solid lines at 400, shaded area at 1200 iterations.

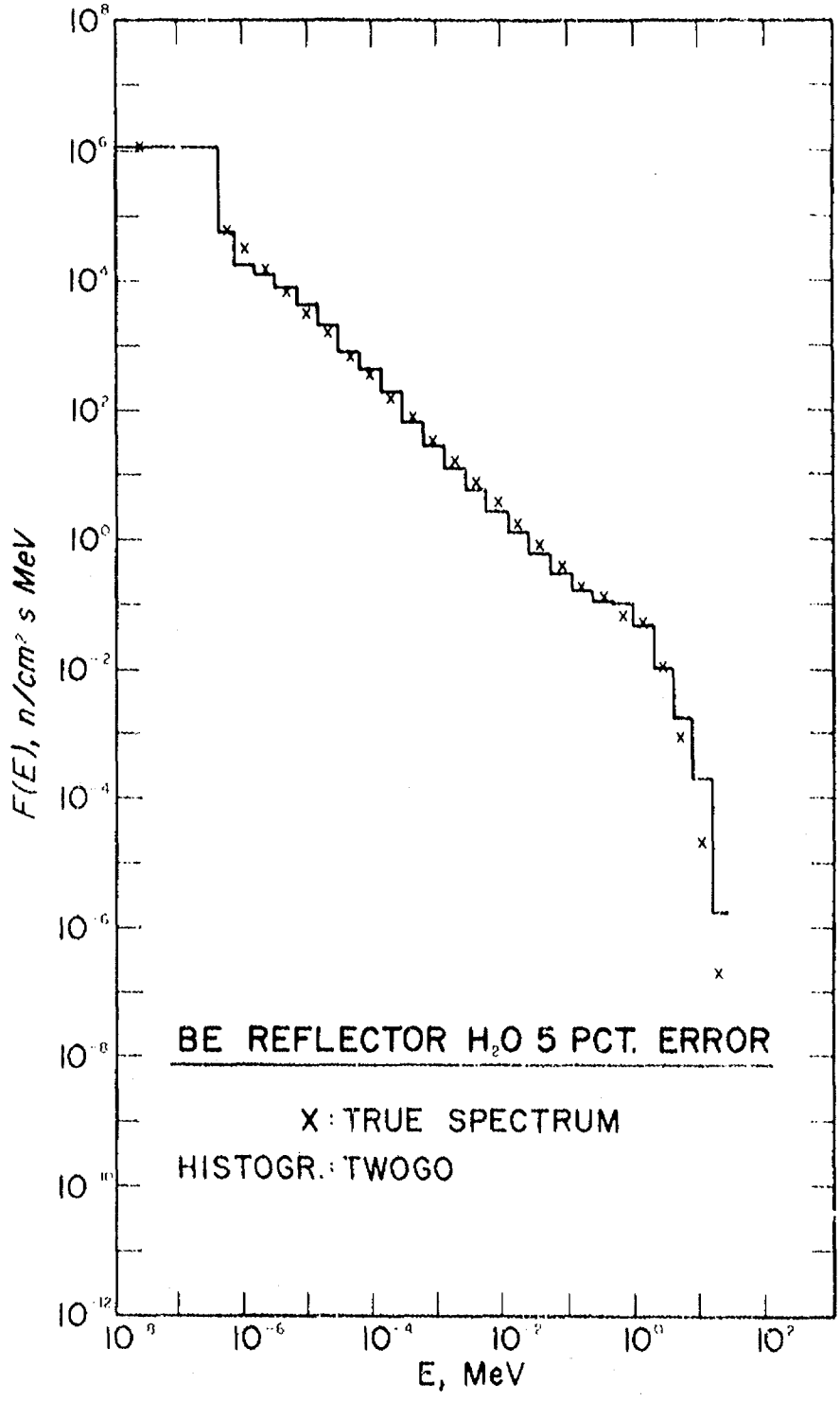

Figure 7. The true and unfolded neutron spectrum in the Be reflector of a homogeneous H_2O reactor. Five percent random errors, Q_2 = 0.02, 200 iterations.

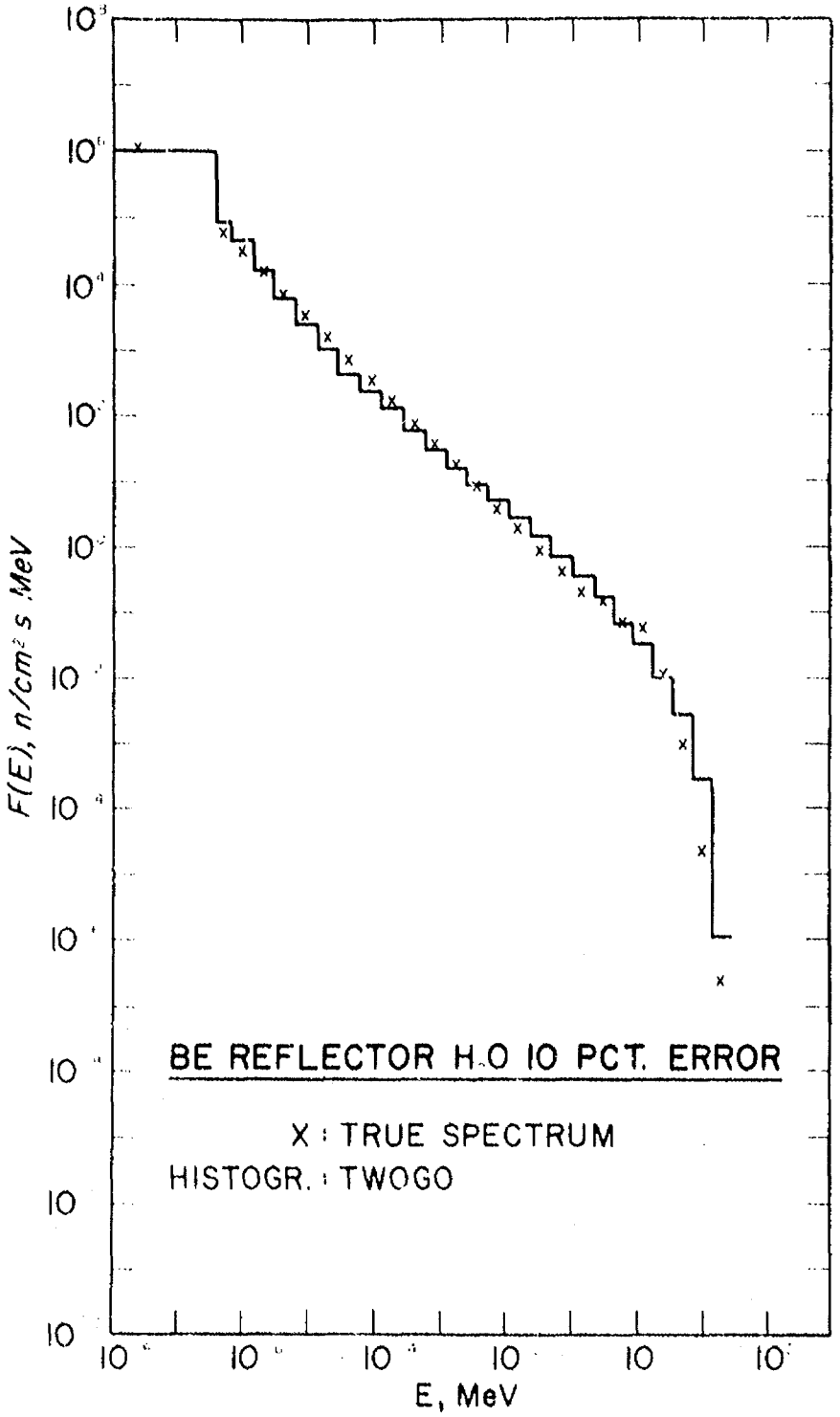

Figure 8. The true and unfolded neutron spectrum in the Be reflector of a homogeneous H_2O reactor. Ten percent random errors, Q_2 = -0.02, 200 iterations.

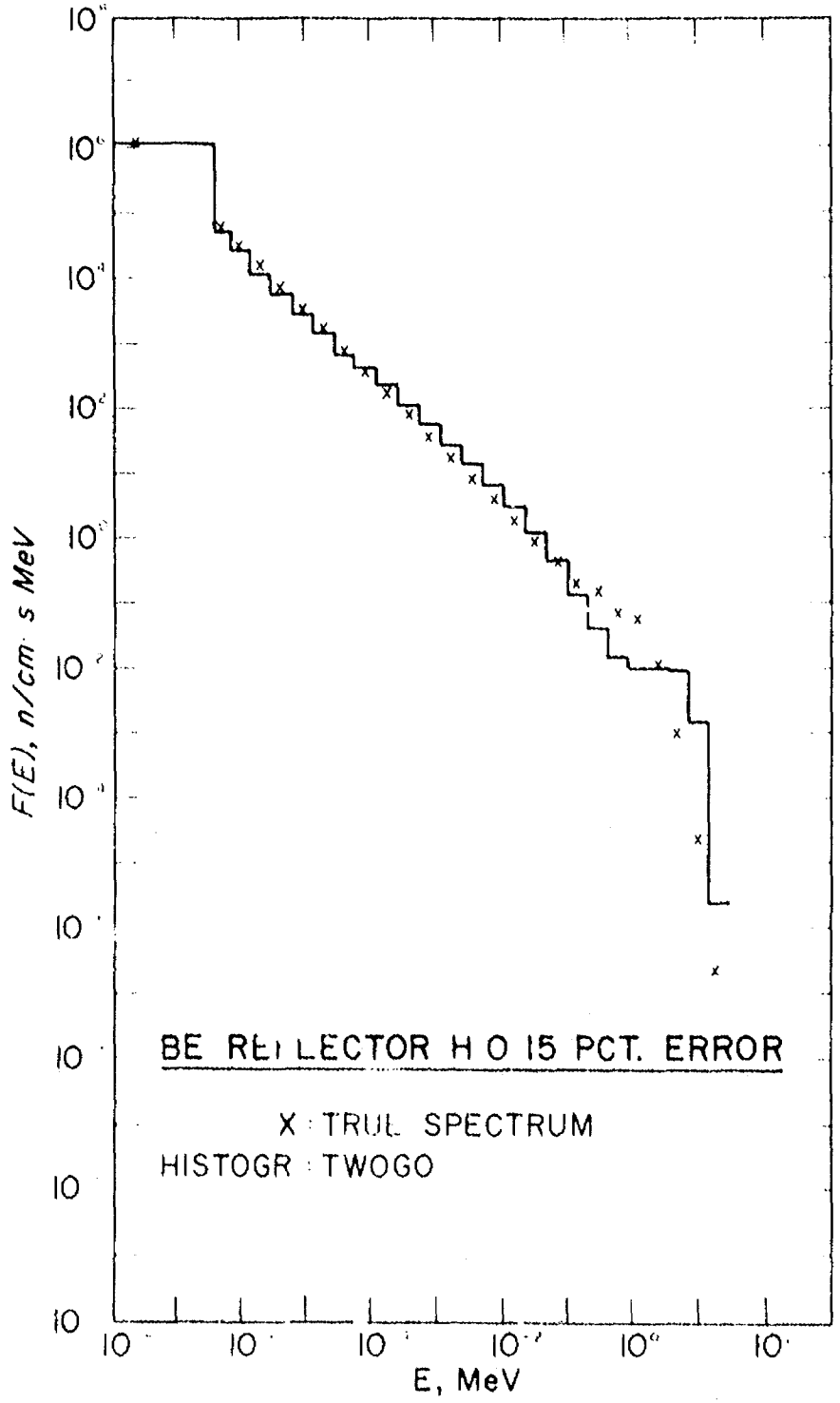

Figure 9. The true and unfolded neutron spectrum in the Be reflector of a homogeneous H_2O reactor. Fifteen percent random errors, Q_2 = 0.02, 200 iterations.

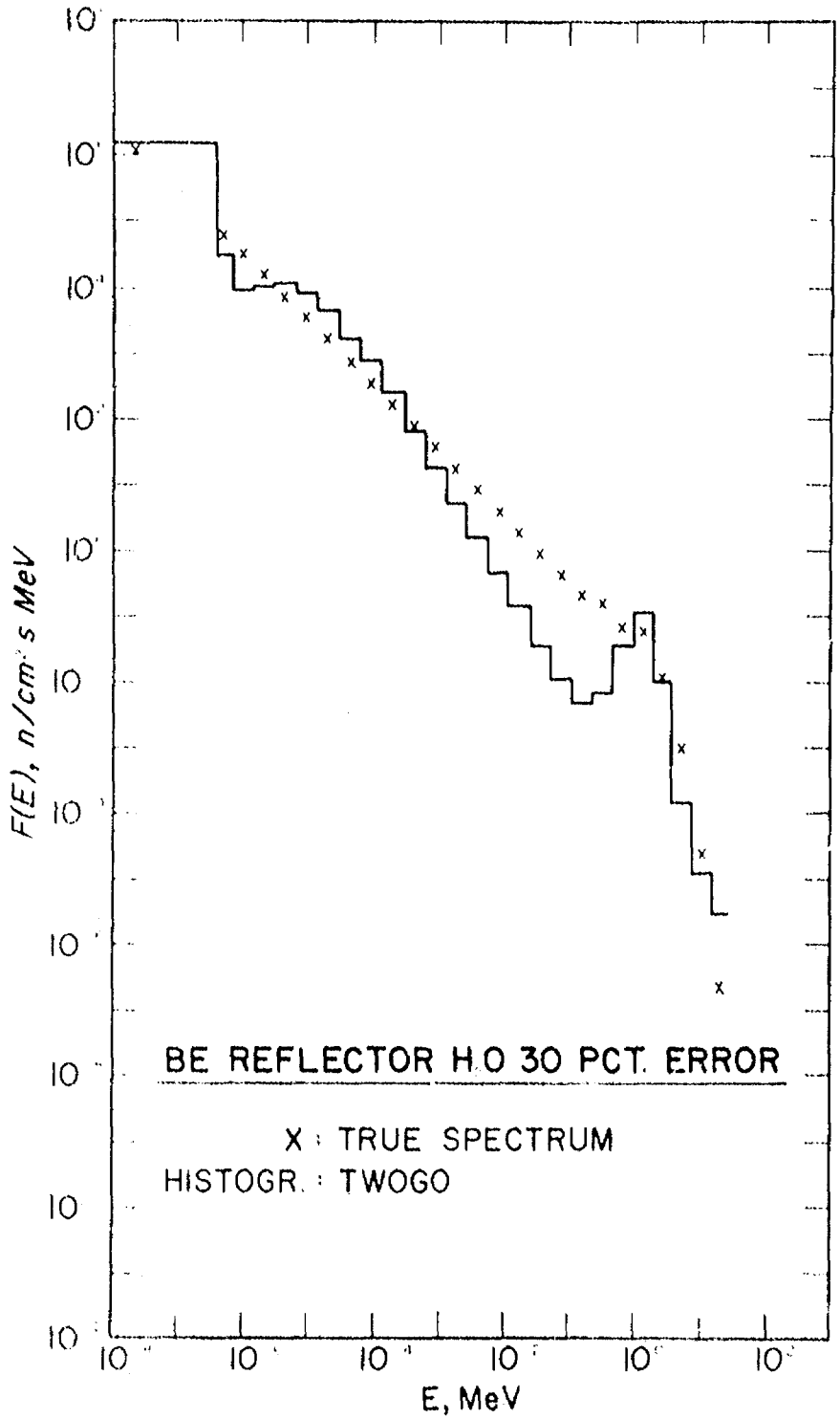

Figure 10. The true and unfolded neutron spectrum in the Be reflector of a homogeneous H_2O reactor. Thirty percent random errors, Q_2 = 0.28, 200 iterations.

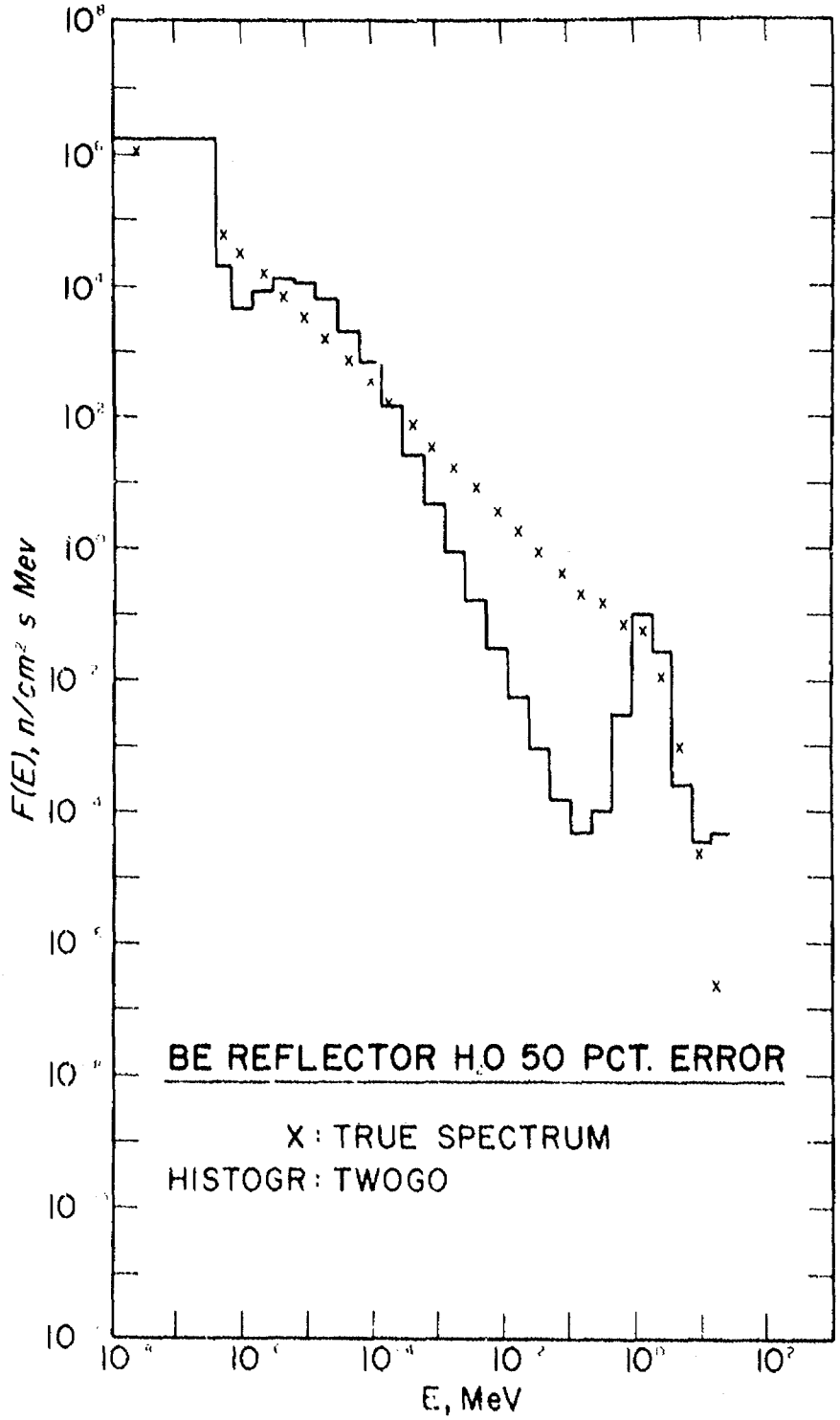

Figure 11. The true and unfolded neutron spectrum in the Be reflector of a homogeneous H_2O reactor. Fifty percent random errors, Q_2 = 0.51, 200 iterations.

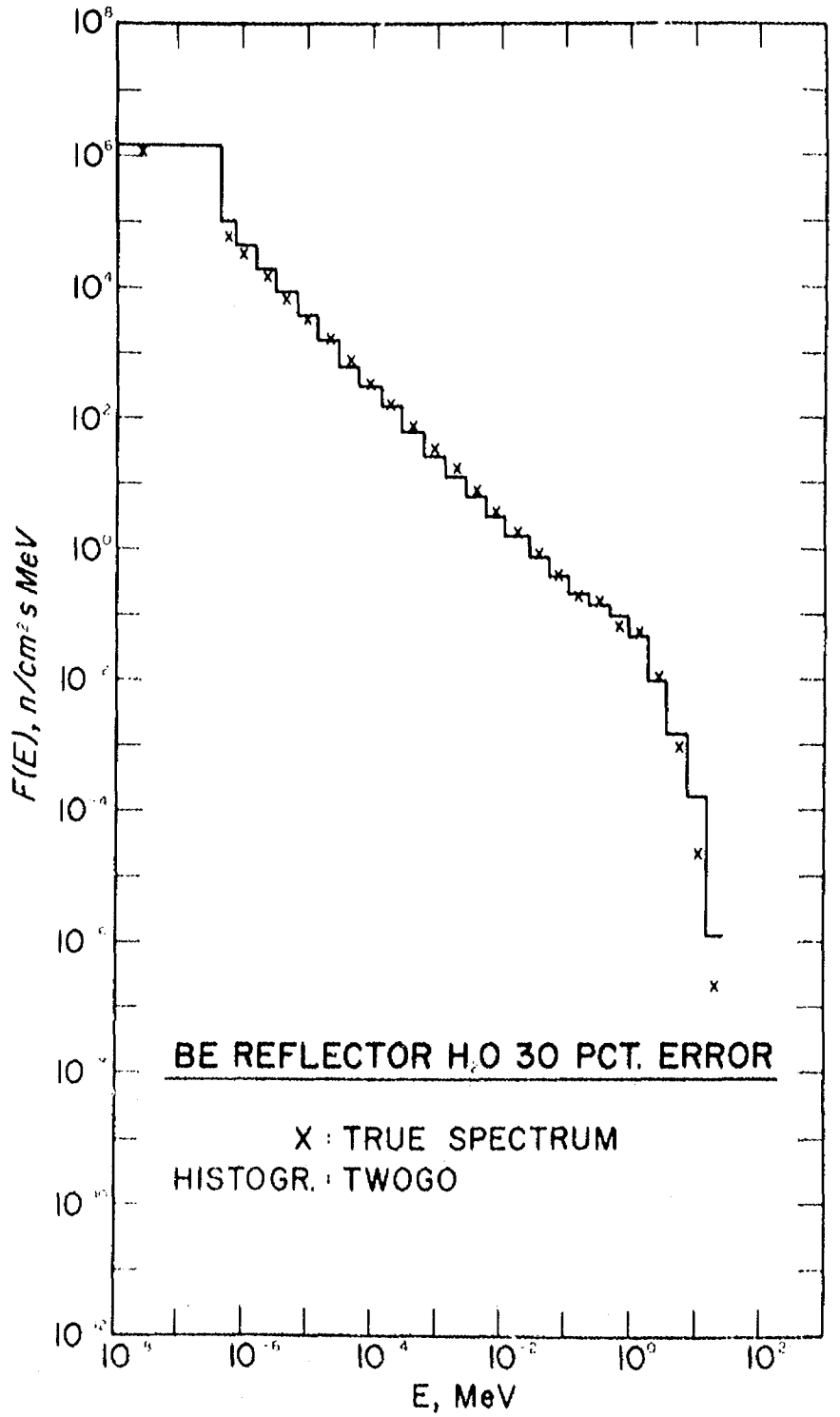

Figure 12. The true and unfolded neutron spectrum in the Be reflector of a homogeneous H_2O reactor. Thirty percent random errors, Q_2 = 0.02, 10 iterations.

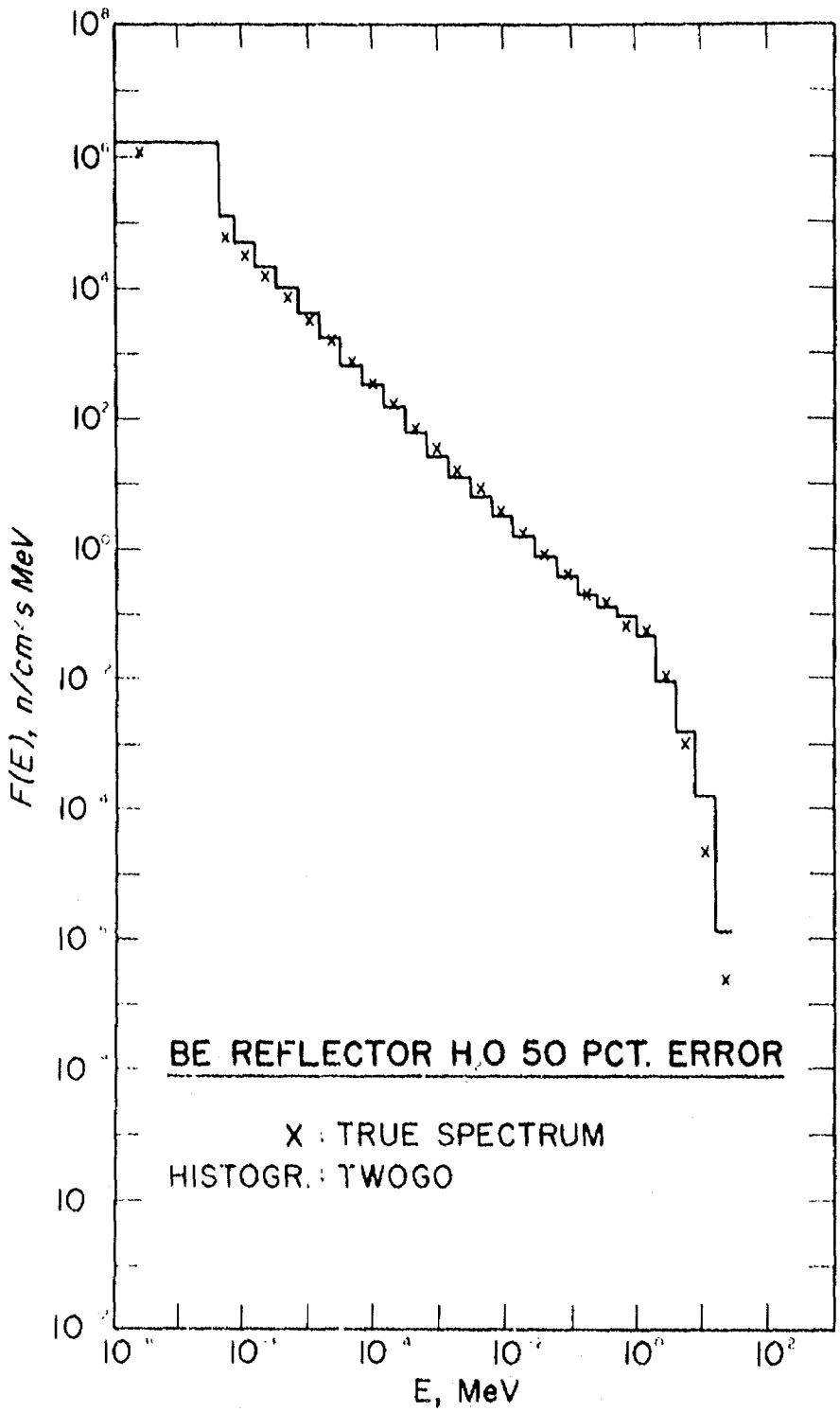

Figure 13. The true and unfolded neutron spectrum in the Be reflector of a homogeneous H_2O reactor. Fifty percent random errors, Q_2 = 0.03, 7 iterations.

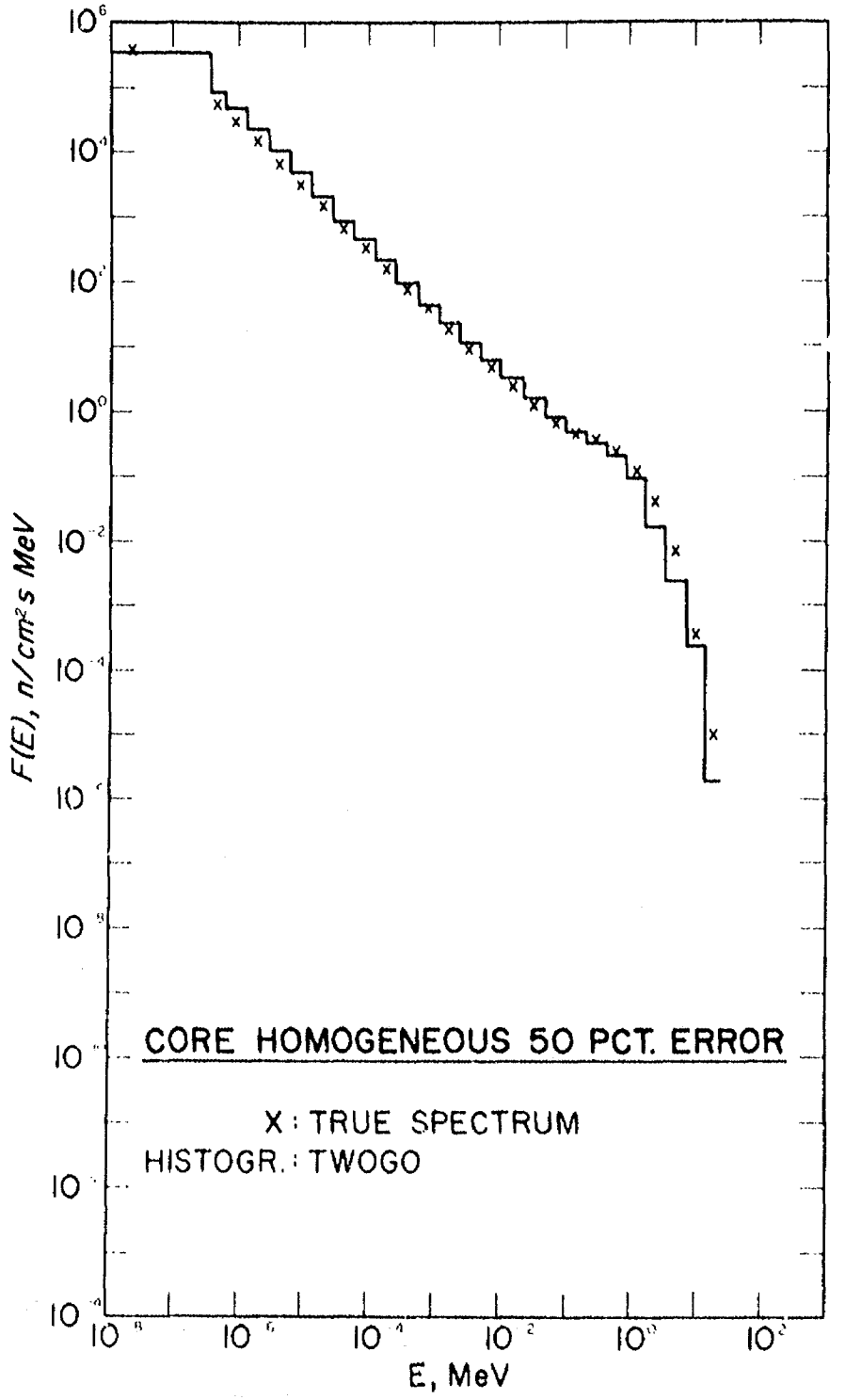

Figure 14. The true and unfolded neutron spectrum in the core of a homogeneous H_2O reactor. Fifty percent random errors, Q_2 = 0, 7 iterations.

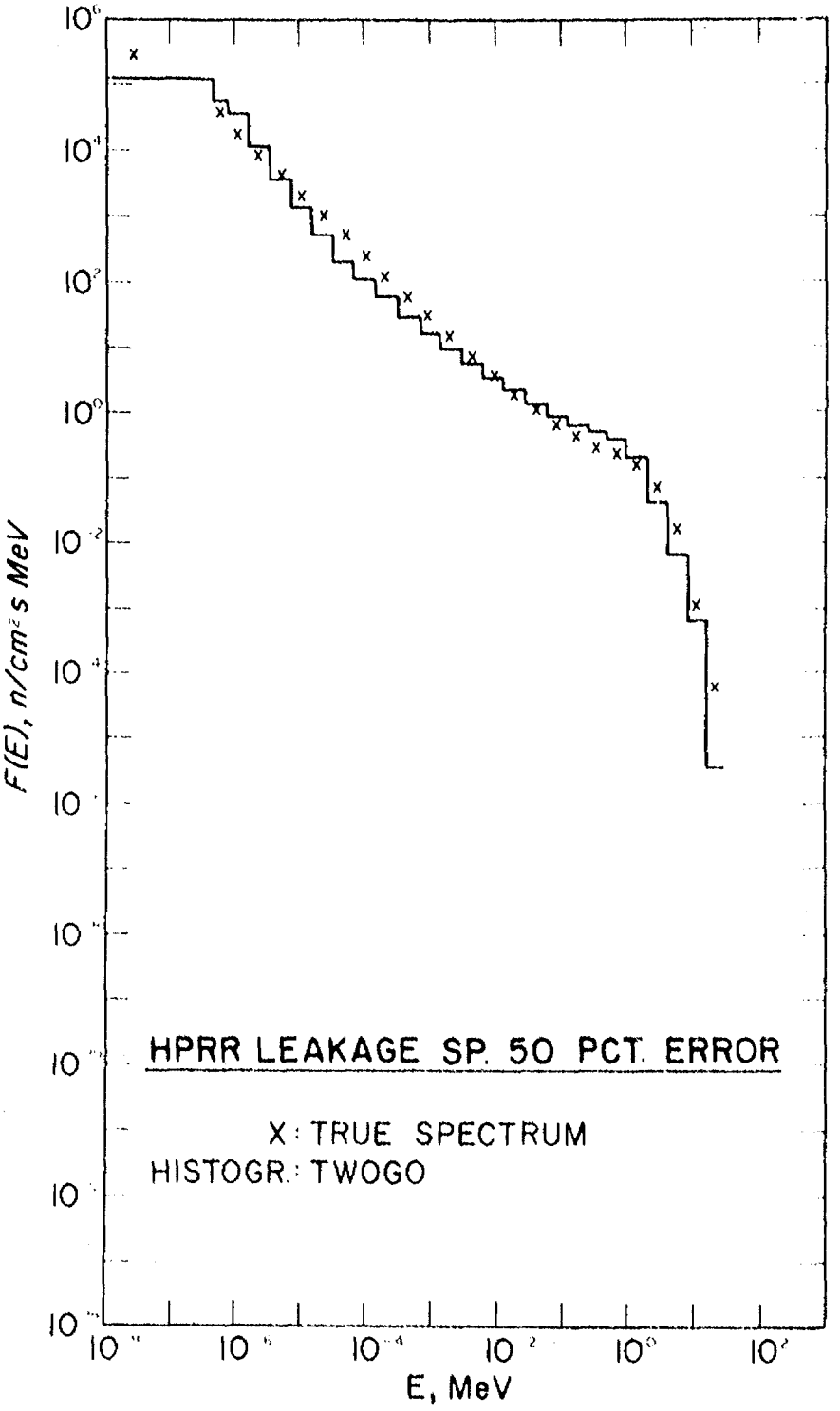

Figure 15. The true and unfolded neutron spectrum of the HPRR leakage spectrum. Fifty percent random errors, $Q_2 = 0$, 12 iterations.

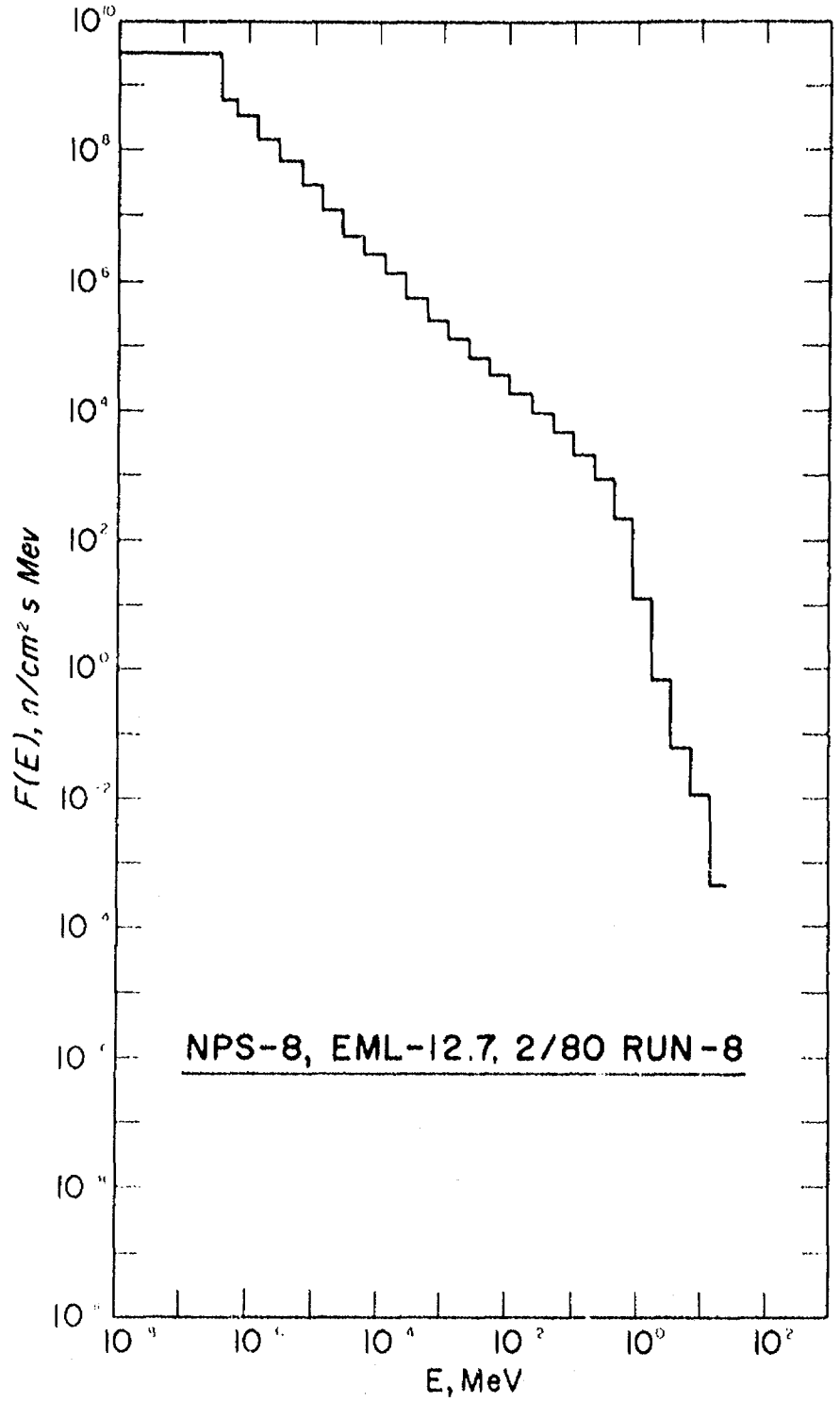

Figure 16. The unfolded neutron spectrum in the containment of NPS-8, location 18. Q_2 = 0.01, 34 iterations.

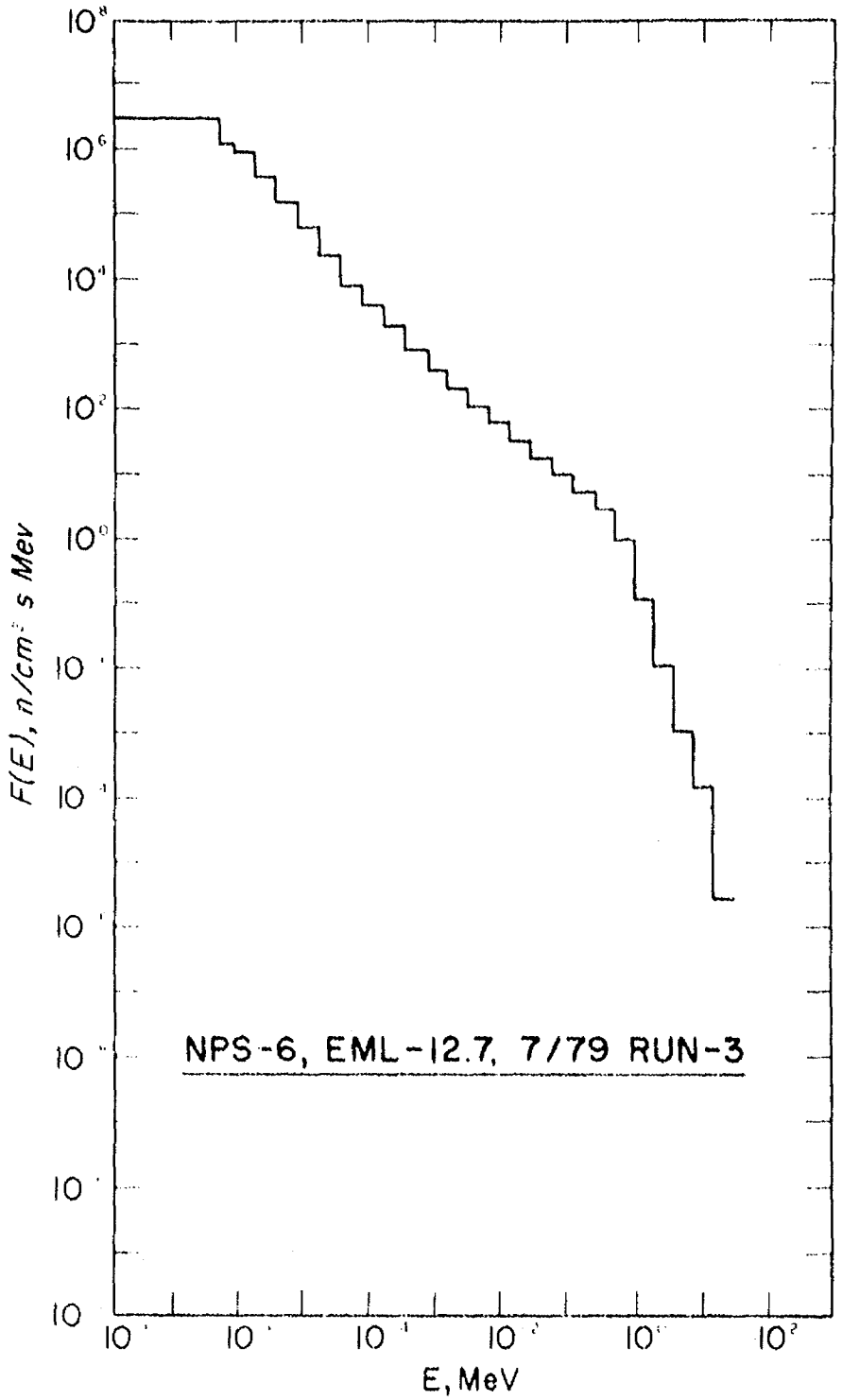

Figure 17. The unfolded neutron spectrum outside the personnel entrance hatch of NPS-6, location 8. Q_2 = 0.04, 18 iterations.

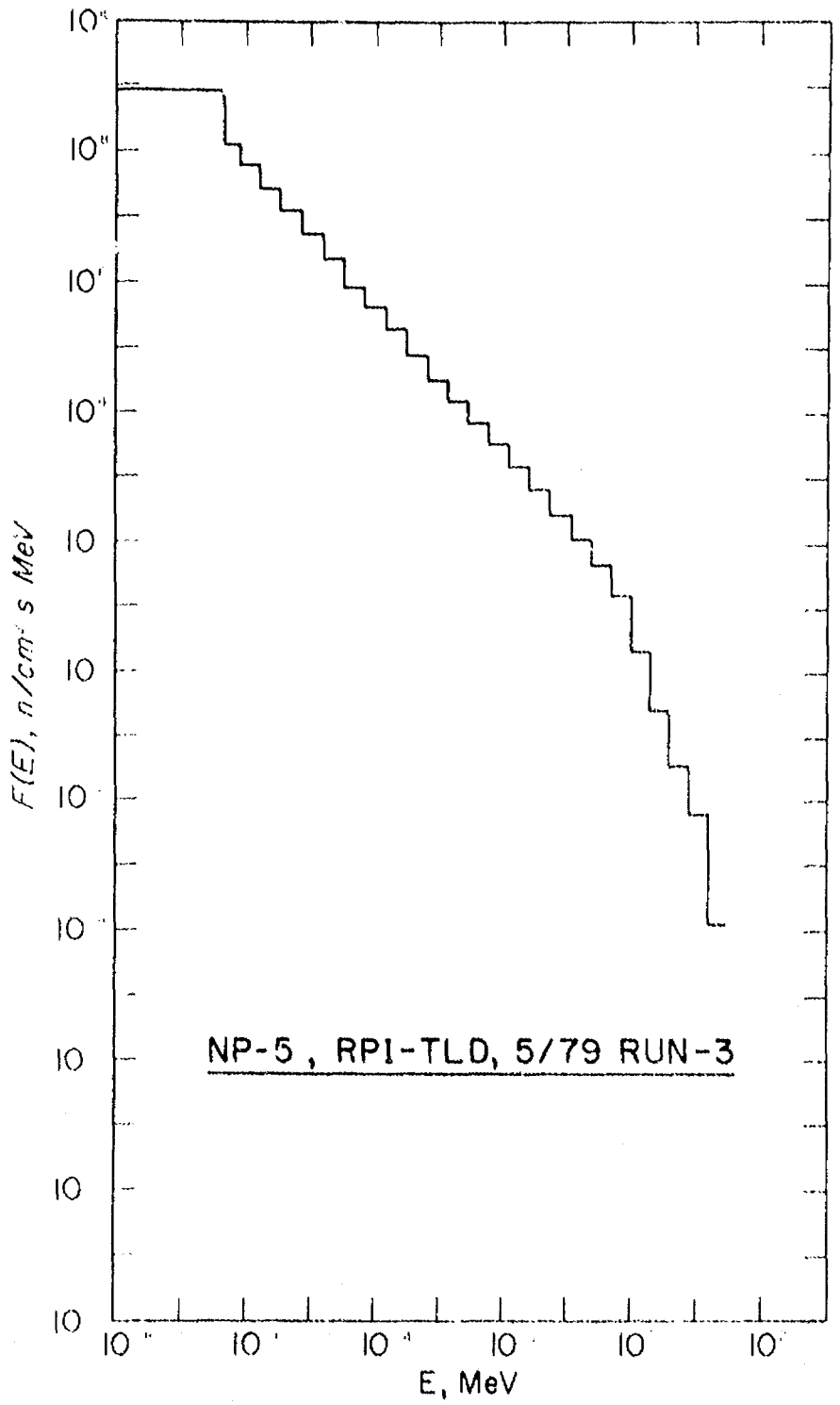

Figure 18. The unfolded neutron spectrum of NPS-5, location 3. Q_2 = 0.01, 26 iterations.